AIP | The Journal of Chemical Physics

Communication: Antibody stability and behavior on surfaces

Derek B. Bush and Thomas A. Knotts IV

Citation: The Journal of Chemical Physics **143**, 061101 (2015); doi: 10.1063/1.4928455
View online: http://dx.doi.org/10.1063/1.4928455
View Table of Contents: http://scitation.aip.org/content/aip/journal/jcp/143/6?ver=pdfcov
Published by the AIP Publishing

Communication: Antibody stability and behavior on surfaces

Derek B. Bush and Thomas A. Knotts IV[a)]
Department of Chemical Engineering, Brigham Young University, Provo, Utah 84602, USA

(Received 11 June 2015; accepted 30 July 2015; published online 11 August 2015)

Antibody microarrays have the potential to revolutionize molecular detection in scientific, medical, and other biosensor applications, but their current use is limited because of poor reliability. It is hypothesized that one reason for their poor performance results from strong antibody-surface interactions that destabilize the antibody structure and create steric interference for antigen recognition. Using a recently developed coarse-grain protein-surface model that has been parameterized against experimental data, antibody-surface interactions for two antibody orientations on two types of surfaces have been investigated. The results show that regardless of attachment geometry, antibodies tend to collapse onto hydrophobic surfaces and exhibit lower overall stability compared to antibodies on hydrophilic surfaces or in bulk solution. The results provide an unprecedented view into the dynamics of antibodies on surfaces and offer new insights into the poor performance exhibited by current antibody microarrays. © *2015 AIP Publishing LLC.* [http://dx.doi.org/10.1063/1.4928455]

I. INTRODUCTION

Antibody (Ab) microarrays have the potential to revolutionize the way that molecular detection is accomplished in fields such as medicine, proteomics, and national defense.[1] They consist of an array of different Abs immobilized to the surface of a chip which, after incubation with a sample of interest, provides information on the concentration of the different constituents of the sample. A single chip can potentially screen hundreds of molecules in parallel in a rapid, inexpensive, and easy-to-use manner that surpasses the abilities of current Ab-based methods of molecular detection such as ELISA.[2–4]

Unfortunately, Ab microarrays have not yet found mainstream use because of excessive variability in their performance.[2,4,5] For example, studies have shown that variability between replicate spots on the same chip can be as high as 43%.[6] This variability comes, in part, from manufacturing imperfections and cross-reactivity;[2,7] however, even under ideal conditions the level of detection can still vary upwards of 1000× from one Ab to the next.[8] Moreover, some Abs lose activity altogether when placed on a surface.[9] In short, better understanding of the factors that affect the behavior of Abs on different types of surfaces is needed to help engineer better Ab microarrays.

One of the difficulties in studying the molecular-level behavior of Abs on surfaces is that no experimental techniques exist to determine the structure of the surface-bound molecule. Typical methods such as X-ray crystallography and NMR cannot be used in heterogeneous environments. Other techniques such as TOF-SIMS (Time-of-Flight Secondary Ion Mass Spectrometry) and FTIR can determine the gross nature of the molecular orientation but do not have the atomic resolution needed to examine the protein structure.[10,11] As such, molecular simulation has emerged as the primary method used when studying protein/surface interactions.[12–16] This work uses molecular simulation to determine how tethering an Ab to different types of surfaces in different orientations affects the stability of the molecule. Specifically, two different orientations (flat and upright) and two types of surfaces (hydrophobic and hydrophilic) have been investigated using the IgG Ab 1IGT.[17]

The Ab/surface system is modeled using a newly developed coarse-grain protein-surface model[18] that has been shown to quantitatively reproduce experimental protein adsorption energies for surfaces of varying hydrophobicity. A coarse-grain implicit solvent model was used because it provides the necessary computational efficiency to sample different Ab configurations with sufficient frequency to calculate accurate thermodynamic averages. The intra-protein interactions are based on the Gō-like model developed by Karanicolas and Brooks.[19,20] The protein-surface interactions are based on a similar forcefield which incorporates the hydrophilicity of each residue and the surface type.

The surface was a flat, homogeneous plane with the Ab placed in the desired orientation 5.8 Å above the surface. A harmonic restraint was placed on the residue closest to the surface to "tether" the molecule to the substrate. In the flat orientation, the entire Ab is laying down on the surface while in the upright orientation the antigen binding sites of the Ab stand away from the surface. All surface/orientation combinations were simulated using the replica exchange method.[21] Simulations were done in the NVT ensemble using the Nosé-Hoover chain integration method and the analysis was done with pyMBAR.[22] Results are presented as heat capacity (C_v) curves, Ab configuration snapshots, and Fab melting temperatures. See the supplementary material for more details on the simulation methods.[23]

Figure 1 depicts the coarse-grain Ab model and the breakdown of the Ab structure as described in the following results (see also Ref. 17). Each sphere represents a single residue. Not labeled in Figure 1 are the white segments, which are short

[a)]Electronic mail: thomas.knotts@byu.edu

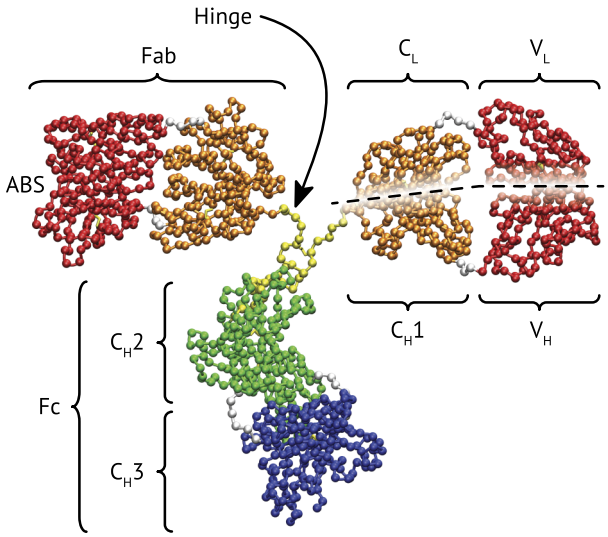

FIG. 1. Depiction of the different segments of the Ab structure discussed in the results.

loops between each of the labeled domains/subdomains. To aid understanding of the Ab behavior, the hydrophobic regions of 1IGT have been highlighted in Figure S1 of the supplementary material.[23]

II. RESULTS

Figure 2 shows the C_v for the Ab as a function of temperature under different conditions. The curves were normalized to make the highest value in each curve equal to one to facilitate comparison of the results from different surface types. The temperature range of Figure 2 is limited to 330 K–390 K because outside of this region the C_v becomes flat. Panel (a) corresponds to the Ab in bulk solution with no surface present (the control), panel (b) the Ab tethered to a hydrophobic surface, and panel (c) the Ab tethered to a hydrophilic surface. In panels (b) and (c) the solid and dashed lines represent tethering in the flat and upright orientations, respectively.

Figure 3 contains representative configurational snapshots of the Ab under different conditions. The time evolution of the radius of gyration for the bulk case is included in Figure S2 of the supplementary material to demonstrate convergence of structures to equilibrium configurations.[23] Panel (a) represents configurations from the Ab in bulk solution, panel (b) represents the Ab tethered to a hydrophobic surface, and panel (c) represents the Ab tethered to a hydrophilic surface. Each configuration has matching roman numeral labels on Figure 2.

The folding behavior shown in panel (a) of Figures 2 and 3 represents the behavior of the Ab in its native aqueous environment. Notice that three peaks are present in the bulk case. This behavior agrees with experimental C_v curves of other Abs[24–26] which have been shown to contain two or three peaks. Before denaturation, the Fabs and Fc domains are free to move and rotate as seen in Figure 3(a)-i. The lowest-temperature peak, located at 353 K, represents the denaturation of the C_H2 subdomains of the Fc domain and the C_H1 and C_L subdomains of the Fabs (Figure 3(a)-ii). The

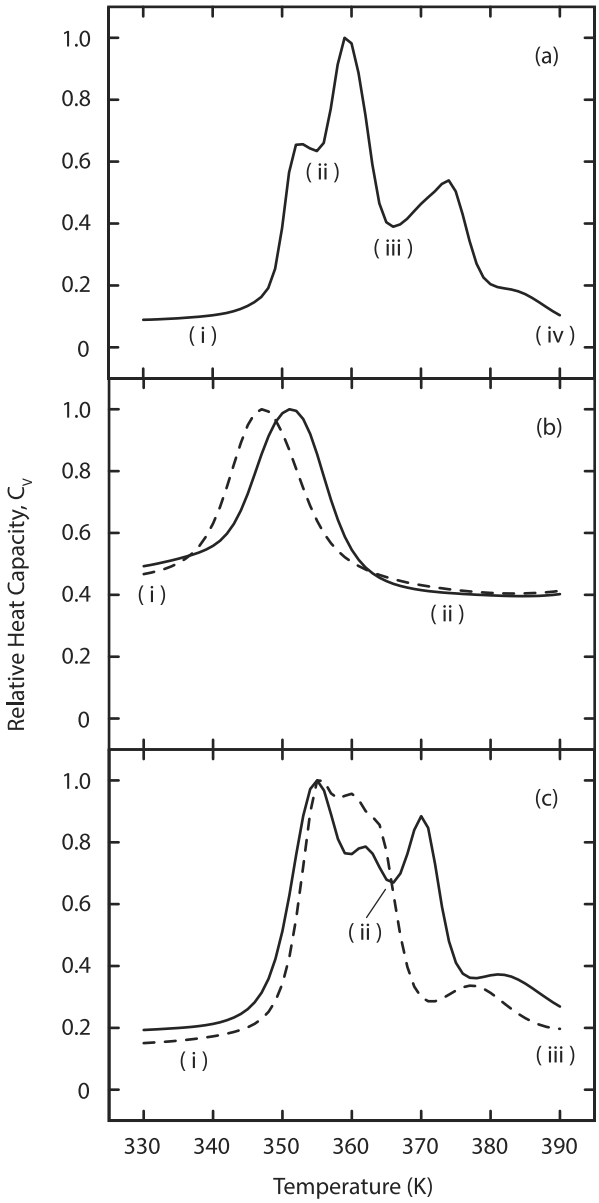

FIG. 2. Relative heat capacity as a function of temperature for the Ab in (a) bulk solution, (b) on a hydrophobic surface, and (c) on a hydrophilic surface. For panels (b) and (c), solid lines represent tethering in a flat orientation and dashed lines represent tethering in an upright orientation. Roman numerals correspond to Ab configurations shown in Figure 3.

tallest peak, located at 359 K, represents the denaturation of all of the V_L and most of the V_H subdomains, which contain the antigen binding sites (Figure 3(a)-iii). The highest-temperature peak, located at 374 K, represents the denaturation of the C_H3 subdomain of the Fc domain, after which the remainder of the V_H subdomains finally denatures (Figure 3(a)-iv).

Panel (b) of Figures 2 and 3 shows the folding behavior of the Ab tethered to a hydrophobic surface. Unlike the bulk case, and regardless of attachment geometry, the C_v curves now show only a single folding transition that contains contributions from the folding behavior of all of the domains in the Ab. The peak occurs at 351 K for the flat orientation and 347 K for the upright orientation. The simplified folding behavior and decreased overall stability of the Ab results from the destabilization of the V_L, V_H, and C_H3 subdomains

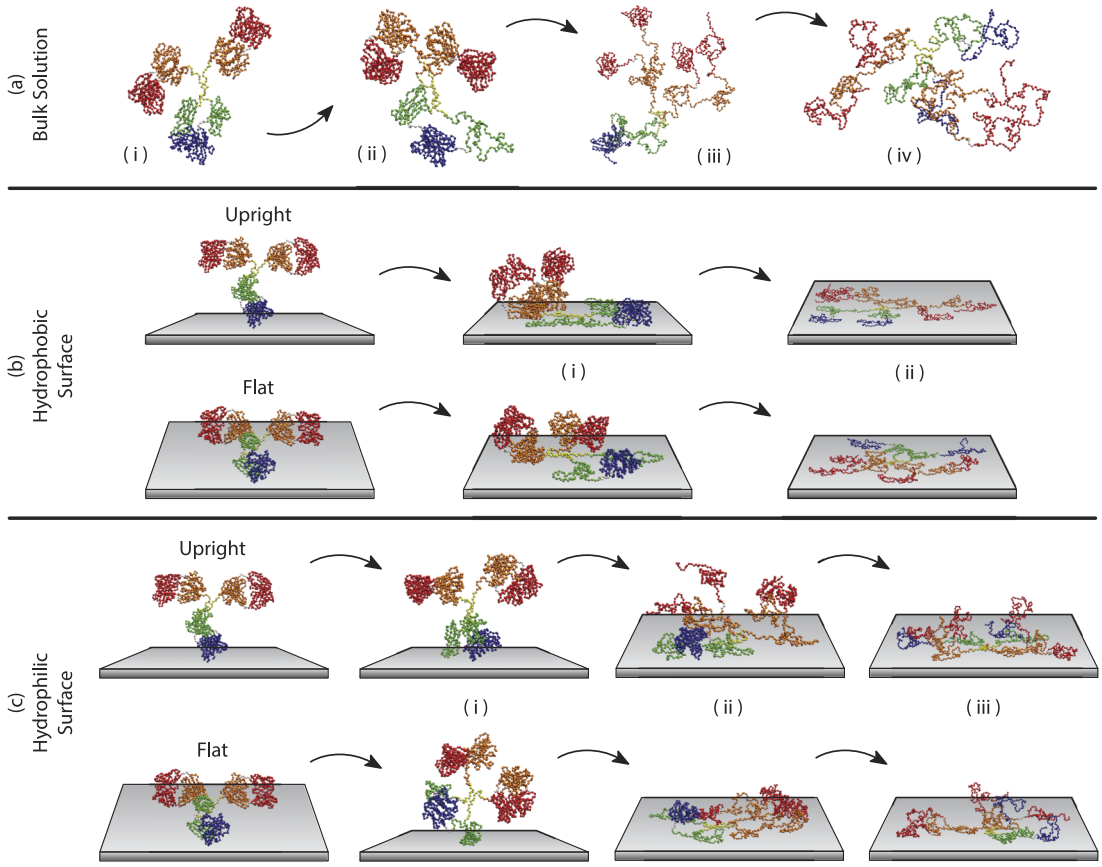

FIG. 3. Representative configurational snapshots of the Ab on different surface types.

which causes them to denature at the same time as the weaker subdomains C_L, C_H1, and C_H2, which themselves have also been destabilized (compared to the bulk case) by attraction to the surface. Figure 3 shows that regardless of the attachment geometry of the Ab, the molecule ultimately adopts a collapsed conformation where the C_H2 subdomains have denatured and are adsorbed on the surface (Figure 3(b)-i). The data show that denatured portions of the Ab have a strong affinity for the hydrophobic surface. At higher temperatures, the entire molecule adsorbs flat onto the surface (Figure 3(b)-ii).

Panel (c) of Figures 2 and 3 shows the folding behavior of the Ab tethered to a hydrophilic surface. When the Ab is tethered in a flat orientation, the folding behavior of the different subdomains becomes distinct from one another similar to the behavior in bulk solution. Four peaks are found in the C_v curve, located at 355 K, 362 K, 370 K, and a final shallow peak at 381 K. The first peak corresponds to the denaturation of most of the Fabs and all of the C_H2 subdomains (Figure 3(c)-ii), the second and fourth peaks the denaturation of the V_H subdomains, and the third peak the denaturation of the C_H3 subdomains. Figure 3(c)-i shows that at lower temperatures the Ab maintains its tertiary structure and has more freedom of movement compared to the Ab on the hydrophobic surface. In contrast to the hydrophobic surface, denatured parts of the molecule are not tightly adsorbed onto the surface and can easily move away from the substrate bulk phase (Figure 3(c)-iii). This change in behavior is due to the decreased attractiveness between the hydrophilic surface and the Ab compared to the hydrophobic surface. The C_v curve of the Ab in the upright position continues to have a single, though broad, peak located at 355 K, but a low peak at 377 K is also present. The broadness of the peak at 355 K indicates that most of the individual domains comprising the Ab fold over a more narrow temperature range than in bulk solution. The peak at 377 K corresponds to the folding of a portion of the V_H subdomains that are stable at high temperatures.

Because Ab microarrays function on the principle of antigen binding, the stability of the antigen binding sites (ABS) of the Fabs on the surface is of paramount importance. Figure 4

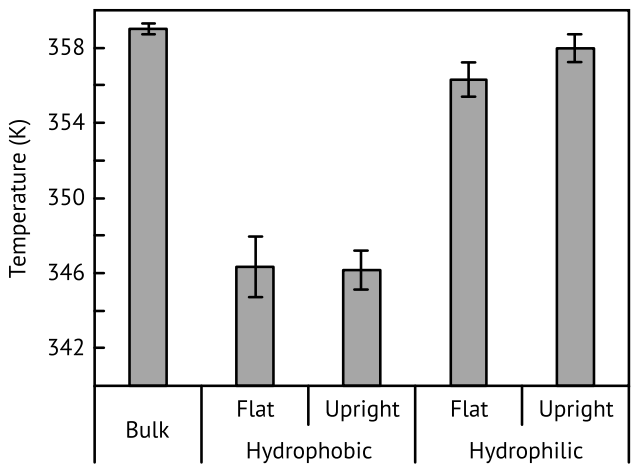

FIG. 4. Melting temperatures of the ABS under different conditions. Error bars represent standard errors from six simulation replicates.

depicts the melting temperature of the ABS. The ABS were considered melted when 50% of the native contacts in the V_L subdomains were broken. See the supplementary material for more details on how the melting temperatures were calculated.[23]

When no surface is present, the ABS melt at 359 K. However, when the Ab is placed on a hydrophobic surface the melting temperature dramatically decreases to 346 K for both the flat and upright orientations. Moreover, to within statistical error, the stability of the ABS on the surface is the same regardless of attachment geometry. The stabilities of the ABS for the flat and upright tethering are similarly equal on the hydrophilic surface, but in contrast to the hydrophobic surface the ABS on a hydrophilic surface are almost as stable as they are in the bulk.

III. DISCUSSION

The hypothesis of this work was that *interactions between surfaces and Abs disrupt Ab structure, which contributes at least partly to the poor performance of current Ab microarrays*. The results indicate that Ab stability is a strong function of surface hydrophobicity, but not attachment geometry. This stands in contrast to previous work showing that the stability of small proteins on surfaces is strongly affected by the placement of the tether. For small proteins, the entire molecule is close to the surface and this close proximity impacts the rotational and vibrational freedom of the entire molecule.[12,13] In contrast, the size of the Ab and the flexible loops that connect the Fabs and Fc domains impart a high degree of rotational and vibrational freedom even when tethered to the surface. Rotational and vibrational freedom also correlate to the changes in stability among different types of surfaces. The decreased attraction between the hydrophilic surface and the Ab, compared to the hydrophobic surface, allows most of the molecule to move freely above the surface. In contrast, the stronger attraction between the hydrophobic surface and the Ab encourages the weaker C_H2 subdomains to denature and become adsorbed onto the surface, which in turn causes the entire molecule to remain close to the surface. As has been reported elsewhere,[13,27,28] the result is a decrease in stability driven by the system desiring to access rotational and vibrational states that are not available until unfolding provides increased conformational freedom.

Perhaps the most important result is that the Ab tends to collapse onto the hydrophobic surface even at temperatures below the main melting transition of the Ab. This insight is significant because it contradicts the notion that when tethered in an upright position the Ab *stays* in a more stable or more accessible conformation.[29] Collapse occurs because some portion of the structure, usually the C_H2 subdomains, partially denatures and then becomes adsorbed onto the surface. The destabilization of the Ab and the subsequent adsorption of the random coil state on the surface may explain some of the reasons for the unreliable performance of Ab microarrays. Unfolding and adsorption of the Ab onto and steric hinderance from the surface likely disrupts antigen recognition and binding. In this case, antigens would need to maneuver to the surface to interact with Fabs that are restricted to move in the plane of the surface. Moreover, extensive denaturation could lead to a loss of function of the Fabs or non-specific binding of proteins. The latter occurs because the surface becomes more attractive to proteins in solution as denatured Ab coils cover it. In short, several mechanisms leading to decreased and highly variable signals from Ab microarray spots are supported by the results.

In light of this, the data suggest that Ab microarray performance could be improved by using a hydrophilic substrate. Traditionally, hydrophobic surfaces are used as deposition of Abs is easily done by spotting. Using a hydrophilic surface would require site-specific covalent linkage of the Abs to the surface to prevent leaching during microarray storage and use. Recent developments are making this highly controlled covalent tethering possible,[30] and future work in this area is promising.[31]

In summary, this work was done to investigate how surface hydrophobicity and tether orientation affect the overall stability of Abs to aid Ab microarray design. The results show that surfaces can have a dramatic effect on the folding behavior and stability of Abs while the attachment geometry has little impact due to the size and flexibility of the molecule. The individual domains of Abs collapse onto and denature more easily on hydrophobic surfaces but are more likely to desorb and remain stable on hydrophilic surfaces.

ACKNOWLEDGMENTS

The authors are grateful for funding from the National Science Foundation (NSF) (No. CBET-1054867) and for computer resources from the Fulton Supercomputing Laboratory at Brigham Young University.

[1]O. Sadik, W. Land, and J. Wang, Electroanalysis **15**, 1149 (2003).
[2]A. A. Ellington, I. J. Kullo, K. R. Bailey, and G. G. Klee, Clin. Chem. **56**, 186 (2010).
[3]B. H. Garcia II, A. Hargrave, A. Morgan, G. Kilmer, E. Hommema, J. Nahrahari, B. Webb, and R. Wiese, J. Biomol. Tech. **18**, 245 (2007).
[4]P. Pavlickova, E. Schneider, and H. Hug, Clin. Chim. Acta **343**, 17 (2004).
[5]I. Balboni, S. M. Chan, M. Kattah, J. D. Tenenbaum, A. J. Butte, and P. J. Utz, Annu. Rev. Immunol. **24**, 391 (2006).
[6]P. Angenendt, J. Glokler, J. Sobek, H. Lehrach, and D. Cahill, J. Chromatogr. A **1009**, 97 (2003).
[7]P. Angenendt, Drug Discovery Today **10**, 503 (2005).
[8]A. Hucknall, D.-H. Kim, S. Rangarajan, R. T. Hill, W. M. Reichert, and A. Chilkoti, Adv. Mater. **21**, 1968 (2009).
[9]P. Angenendt, J. Glokler, D. Murphy, H. Lehrach, and D. J. Cahill, Anal. Biochem. **309**, 253 (2002).
[10]T. S. Tsapikouni and Y. F. Missirlis, Mater. Sci. Eng. B **152**, 2 (2008).
[11]A. P. Le Brun, S. A. Holt, D. S. Shah, C. F. Majkrzak, and J. H. Lakey, Eur. Biophys. J. **37**, 639 (2008).
[12]S. Wei and T. A. Knotts IV, J. Chem. Phys. **134**, 185101 (2011).
[13]S. Wei and T. A. Knotts IV, J. Chem. Phys. **133**, 115102 (2010).
[14]B. K. Loong and T. A. Knotts IV, J. Chem. Phys. **141**, 051104 (2014).
[15]S.-W. Hung, P.-Y. Hsiao, M.-C. Lu, and C.-C. Chieng, J. Phys. Chem. B **116**, 12661 (2012).
[16]R. B. Pandey, Z. Kuang, B. L. Farmer, S. S. Kim, and R. R. Naik, Soft Matter **8**, 9101 (2012).
[17]L. J. Harris, S. B. Larson, K. W. Hasel, and A. McPherson, Biochemistry **36**, 1581 (1997).
[18]S. Wei and T. A. Knotts IV, J. Chem. Phys. **139**, 095102 (2013).
[19]J. Karanicolas and C. Brooks, J. Mol. Biol. **334**, 309 (2003).
[20]J. Karanicolas and C. Brooks, Protein Sci. **11**, 2351 (2002).

[21]Y. Sugita and Y. Okamoto, Chem. Phys. Lett. **314**, 141 (1999).
[22]M. R. Shirts and J. D. Chodera, J. Chem. Phys. **129**, 124105 (2008).
[23]See supplementary material at http://dx.doi.org/10.1063/1.4928455 for further details on the simulations, model, and analysis methods.
[24]D. Lowe, K. Dudgeon, R. Rouet, P. Schofield, L. Jermutus, and D. Christ, Adv. Protein Chem. Struct. Biol. **84**, 41–61 (2011).
[25]K. Zheng, C. Bantog, and R. Bayer, mAbs **3**, 568 (2011).
[26]N. Chennamsetty, V. Voynov, V. Kayser, B. Helk, and B. L. Trout, Proc. Natl. Acad. Sci. U. S. A. **106**, 11937 (2009).
[27]M. Friedel, A. Baumketner, and J.-E. Shea, Proc. Natl. Acad. Sci. U. S. A. **103**, 8396 (2006).
[28]M. Friedel, A. Baumketner, and J.-E. Shea, J. Chem. Phys. **126**, 095101 (2007).
[29]Y. Jung, J. Y. Jeong, and B. H. Chung, Analyst **133**, 697 (2008).
[30]M. T. Smith, J. C. Wu, C. T. Varner, and B. C. Bundy, Biotechnol. Prog. **29**, 247 (2013).
[31]J. C. Y. Wu, C. H. Hutchings, M. J. Lindsay, C. J. Werner, and B. C. Bundy, J. Biotechnol. **193**, 83 (2015).